



# Polarisation Observables from Strangeness Photoproduction on g9a

CLAS12 International Workshop 2023, Paris



Stuart Fegan  
University of York  
March 22nd, 2023





# Outline

## 1 Introduction

- A World of Polarisation (Observables)
- JLab, CLAS and FROST

## 2 Analysis

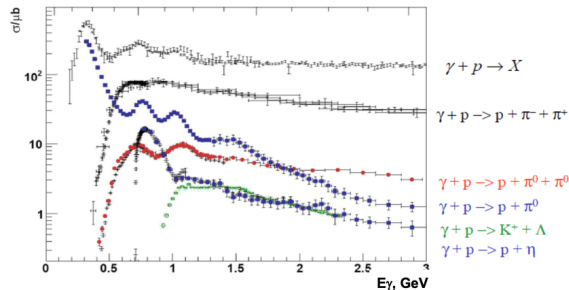
- Event Selection
- Observable Extraction
- Results

## 3 Conclusions and Outlook



## Motivation

- Baryon Spectroscopy is the study of excited nucleon states
- Finding some states can be difficult in a simple “bump hunt”; many are wide and overlap
- Use alternative means; coupling strength to a reaction channel, manifestation in experimental observables, etc. to aid searches



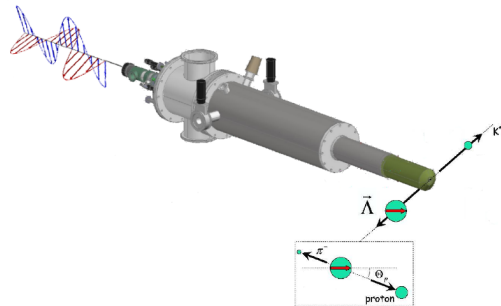
R. Beck and U. Thoma, EPJ Web Conf 134, 04003 (2017)

- Looking for polarisation observables on strangeness photoproduction
- Many possible channels, but this talk will focus on  $K^+\Lambda$ 

$$\gamma p \rightarrow K^+\Lambda \rightarrow K^+p\pi^-$$
- 16 observables for single meson photoproduction, arising from the scattering amplitudes of the interaction and the particles which carry polarisation



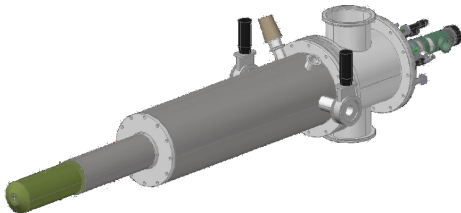
- “Single”:  $\sigma, \Sigma, P, T$
- Beam-Target:  $E, F, G, H$
- Beam-Recoil:  $O_X, O_Z, C_X, C_Z$
- Target-Recoil:  $T_X, T_Z, L_X, L_Z$





## PARA/PERP, Target too

- With a polarised beam and target, can access the single and beam-target double observables
  - Single:  $\sigma, \Sigma, P, T$
  - Beam-Target:  $E, F, G, H$
- And more with recoil (i.e. with a self-analysing hyperon)



This work has two goals:

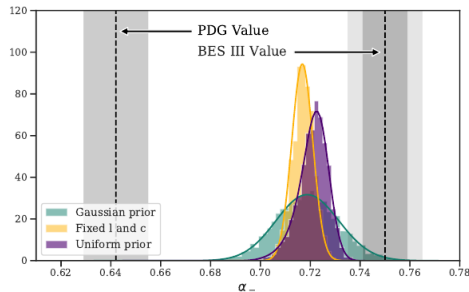
- Verify the beam asymmetry,  $\Sigma$
- Perform first measurements in this channel of the beam-target observable,  $G$



# Identities and Interpretations

Observable	W (MeV)	$\theta$ (deg)	Data	Lab
$d\sigma/d\Omega$	1610-2390	18-162	701	ELSA
	1612-1896	66-143	1306	MAMI
	1617-2290	32-148	920	CEBAF
	1617-2108	26-154	90	ELSA
	1625-2395	27-154	1674	CEBAF
	1628-2533	26-143	1377	CEBAF
$\Sigma$	1934-2310	13-41	78	Spring-8
	1649-1906	31-144	66	GRAAL
	1721-2180	37-134	314	CEBAF
	1946-2300	13-49	45	Spring-8
	1946-2280	13-49	30	Spring-8
P	2041-2238	18-32	4	Spring-8
	1617-2290	26-154	233	CEBAF
	1625-2545	26-143	1497	CEBAF
	1649-1906	31-144	66	GRAAL
	1660-2017	41-139	12	ELSA
T	1660-2280	34-146	30	ELSA
	1721-2180	37-134	314	CEBAF
	1649-1906	31-144	66	GRAAL
$C_{\mathcal{P}}$	1721-2180	37-134	314	CEBAF
	1678-2454	32-139	144	CEBAF
$C_{\mathcal{P}}$	1678-2454	32-139	146	CEBAF
$O_x$	1649-1906	31-144	66	GRAAL
	1721-2180	37-134	314	CEBAF
$O_z$	1649-1906	31-144	66	GRAAL
	1721-2180	37-134	314	CEBAF

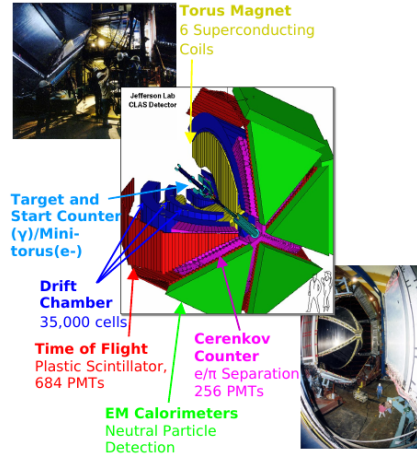
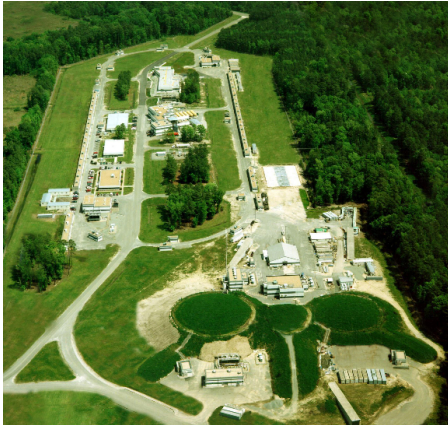
- Polarisation observable data is relatively sparse in  $K^+\Lambda$
- Possible to verify the weak decay parameter,  $\alpha_-$ , using observables and Fierz identities



D.G. Ireland et. al., Phys. Rev. Lett. 123, 182301 (2019)



# N\* Experiments with CLAS

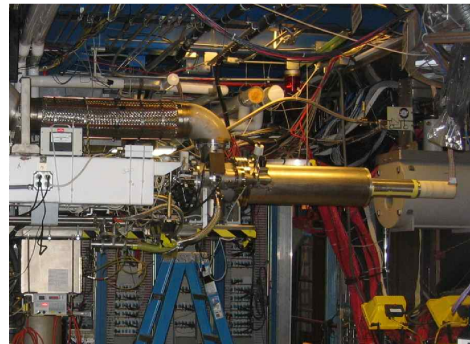


NIM A, 503(3), 2003



- Data from g9a run period: November 2007 to February 2008
- Linearly and circularly polarised photon beams on a longitudinally polarised target
- Polarisation direction regularly flipped during run
- Nine coherent peak settings in linear polarisation, spanning energy range 0.7 to 2.3 GeV
- In this case, the reduced cross section can be expressed as:

$$\frac{d\sigma}{d\Omega} = \sigma_0 \{1 - P_{lin}\Sigma \cos(2\phi) + P_z(P_{lin}G \sin(2\phi))\}$$

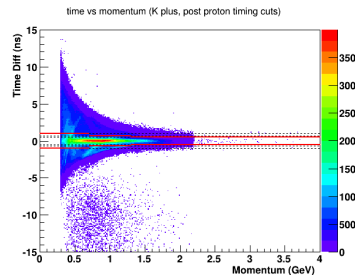
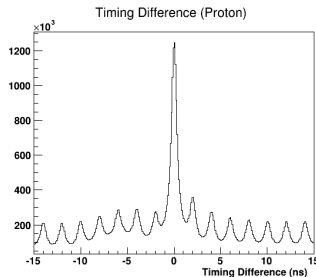
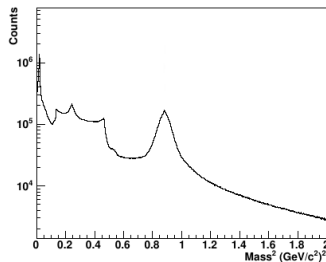






## Analysis - Particle ID

- Initial particle ID via combination of charge and time-of-flight mass
- Select candidate Protons and Kaons
- Apply photon-to-particle timing difference cuts eliminate misidentification



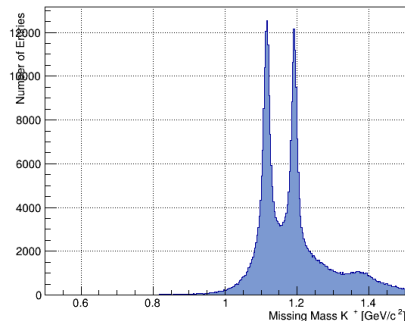
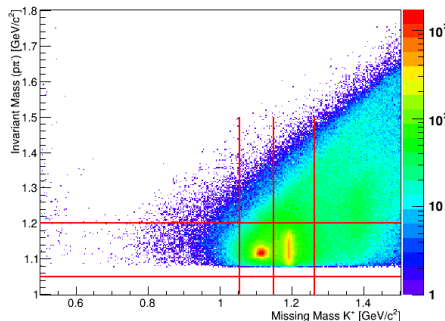


## Channel Identification

- Select channel of interest:

$$\gamma p \rightarrow K^+ \Lambda \rightarrow K^+ p \pi^-$$

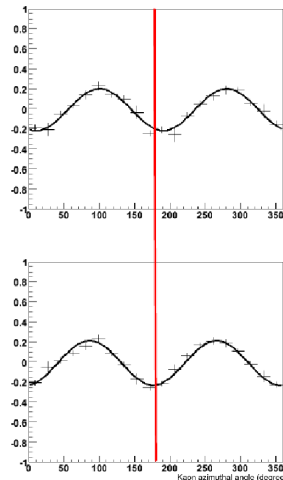
- Non exclusive selection - reconstruct pion from detected proton and kaon
- Hyperons identified via kaon missing mass and proton pion invariant mass





## Extracting Observables

- Binned fitting on asymmetries of two states of beam polarisation (PARA and PERP)
- Technique has been extensively employed in the JLab N\* program and similar experiments worldwide
- Recall that on a linpol beam and a longitudinally polarised target:
$$\frac{d\sigma}{d\Omega} = \sigma_0 \{1 - P_{lin} \Sigma \cos(2\phi) + P_z (P_{lin} G \sin(2\phi))\}$$
- A  $\cos(2\phi) + \sin(2\phi)$  fit to a PARA/PERP asymmetry can be used to extract  $\Sigma$  and  $G$  for each state of target polarisation





## Extracting Observables II

- Binned asymmetry fitting relies on a number of assumptions
- In lower statistics channels, or datasets where PARA and PERP have large variations between them in flux, polarisation, etc., reliable observable extraction is more challenging
- Using a maximum likelihood approach, we can extract observables event-by-event, and better account for variation between polarisation states
- We can define the likelihood function for each event as:

$$L_i = c_i[1 - P_{lin,i}\Sigma\cos(2\phi_i) + P_{z,i}(P_{lin,i}G\sin(2\phi_i))]A$$

- And extract observables by maximising the log-likelihood function:

$$\log L = b + \sum_i \log[1 - P_{lin,i}\Sigma\cos(2\phi_i) + P_{z,i}(P_{lin,i}G\sin(2\phi_i))]$$



## Dilution of Observables

- Parameters extracted from  $\cos(2\phi) + \sin(2\phi)$  fits are the free proton value, diluted with a carbon contribution (and beam and target polarisations)
- i.e. for the  $\Sigma$  observable, we actually measure  $\Sigma_{Butanol}$ , from which we can infer the free proton value

$$\Sigma_{Proton} = \frac{1}{N_{Proton}} (N_{Butanol} \Sigma_{Butanol} - N_{Carbon} \Sigma_{Carbon})$$

- For G, carbon in the target is unpolarised and we measure  $G_{Butanol}$ , estimating the free proton value via;

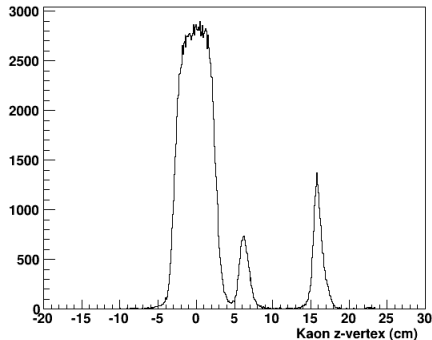
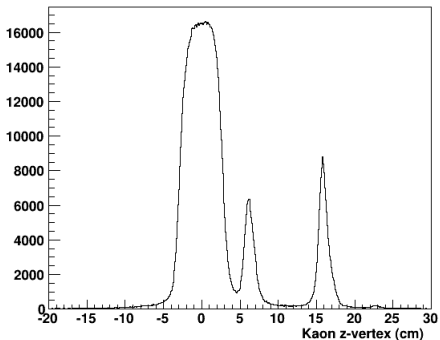
$$G_{Proton} = \frac{N_{Butanol}}{N_{Proton}} (N_{Butanol} G_{Butanol})$$

- The 'N' terms represent event yields per bin corresponding to the relevant material
- These must be estimated for Carbon and Proton...



## Target Selection

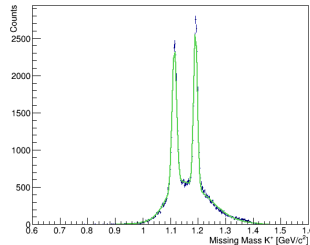
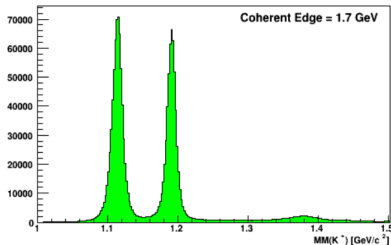
- FROST target contains Butanol (left), Carbon (centre) and Polythene (right)
- Resolvable from Kaon z-vertex after particle and channel identification



- Only Butanol is polarised, other targets used to account for nuclear background and dilution effects of unpolarised nuclei in butanol



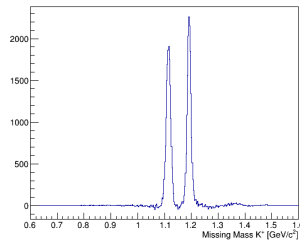
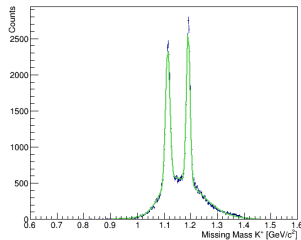
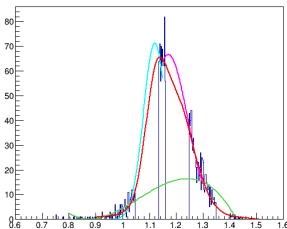
## Estimating Carbon



- Controlling systematic uncertainties, particularly on a measurement of  $G$ , requires a robust method of accounting for Carbon
- We know from data on proton targets (left) that shape under the hyperon peaks on butanol (right) is almost entirely from bound nucleon effects



# Estimating Carbon



- Parameterise, using carbon data to initialise a fit
- Refit to Butanol and determine proportion of Carbon events in each bin





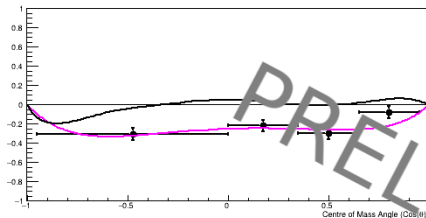
## Initial Results

- Initial results from the maximum likelihood technique for the  $G$  observable on  $K^+\Lambda$
- Comparison to Bonn-Gatchina (pink line) and Jülich Bonn (black line) model predictions (from 2017)

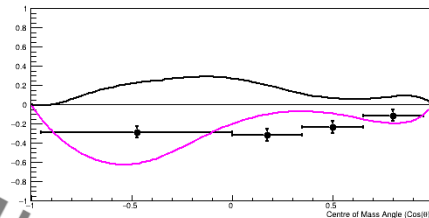


# Initial Results, G

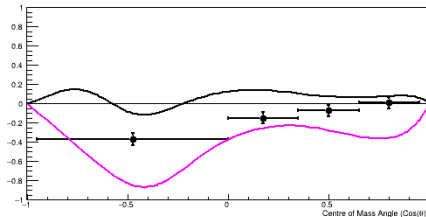
G for  $K\Lambda$  at  $W = 1.77$  to  $1.87$  GeV



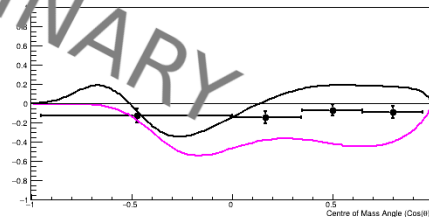
G for  $K\Lambda$  at  $W = 1.87$  to  $1.97$  GeV



G for  $K\Lambda$  at  $W = 1.97$  to  $2.06$  GeV

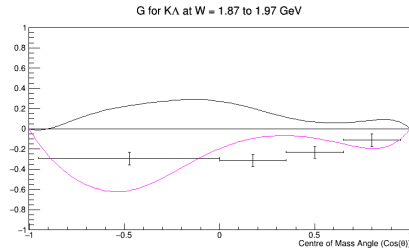
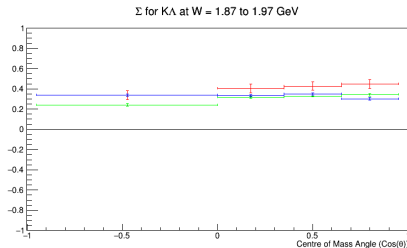


G for  $K\Lambda$  at  $W = 2.06$  to  $2.15$  GeV





## Outlook and Plans

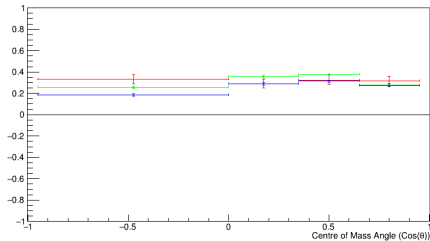


- First (preliminary) measurement of the G observable for  $K^+\Lambda$  photoproduction using maximum likelihood technique on this data
- Final systematic checks in progress
- Data allows  $K^+\Lambda$  and  $K^+\Sigma$  channels to be studied
- Measuring target-recoil observables may be feasible using this method

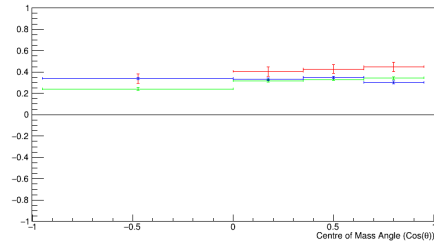


# Initial Results, $\Sigma$

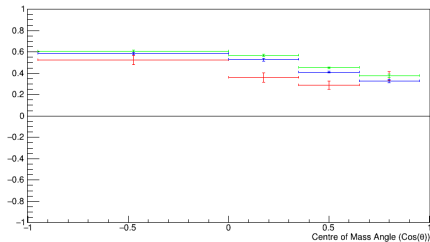
$\Sigma$  for  $K\Lambda$  at  $W = 1.77$  to  $1.87$  GeV



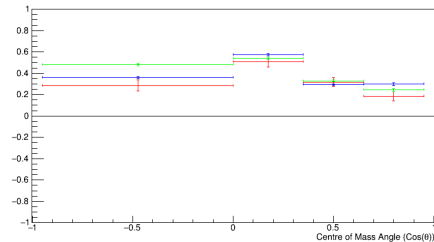
$\Sigma$  for  $K\Lambda$  at  $W = 1.87$  to  $1.97$  GeV



$\Sigma$  for  $K\Lambda$  at  $W = 1.97$  to  $2.06$  GeV



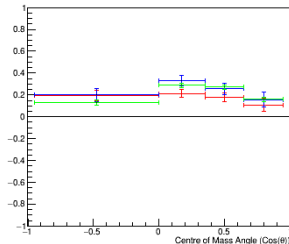
$\Sigma$  for  $K\Lambda$  at  $W = 2.06$  to  $2.15$  GeV



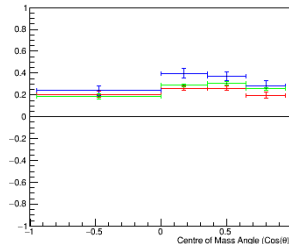


# (Backup) Binned Asymmetry extraction, $\Sigma$

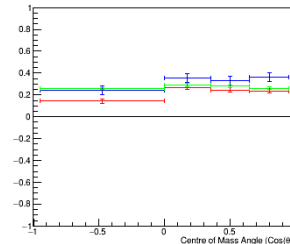
$\Sigma$  comparison for  $K\Lambda$  at  $W = 1.66$  to  $1.77$  GeV



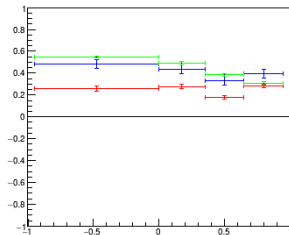
$\Sigma$  comparison for  $K\Lambda$  at  $W = 1.77$  to  $1.87$  GeV



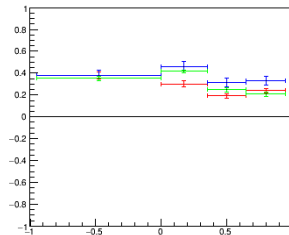
$\Sigma$  comparison for  $K\Lambda$  at  $W = 1.87$  to  $1.97$  GeV



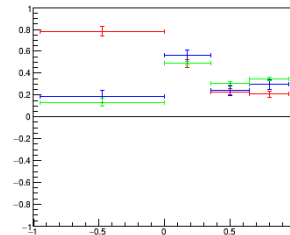
$\Sigma$  comparison for  $K\Lambda$  at  $W = 1.97$  to  $2.06$  GeV



$\Sigma$  comparison for  $K\Lambda$  at  $W = 2.06$  to  $2.15$  GeV



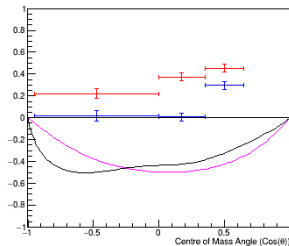
$\Sigma$  comparison for  $K\Lambda$  at  $W = 2.15$  to  $2.24$  GeV



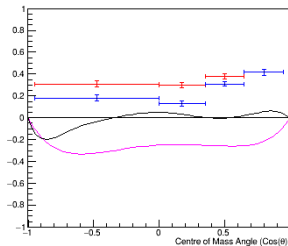


# (Backup) Binned Asymmetry extraction, G

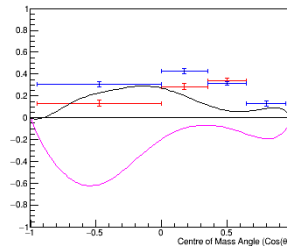
G for  $K\Lambda$  at  $W = 1.67$  to  $1.77$  GeV



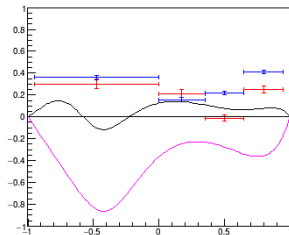
G for  $K\Lambda$  at  $W = 1.77$  to  $1.87$  GeV



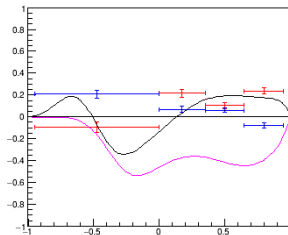
G for  $K\Lambda$  at  $W = 1.87$  to  $1.97$  GeV



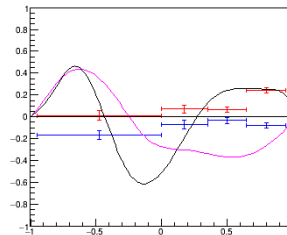
G for  $K\Lambda$  at  $W = 1.97$  to  $2.06$  GeV



G for  $K\Lambda$  at  $W = 2.06$  to  $2.15$  GeV



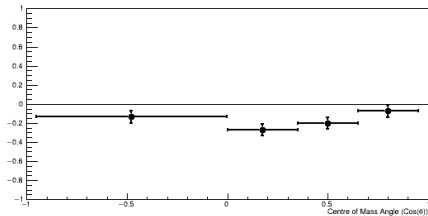
G for  $K\Lambda$  at  $W = 2.15$  to  $2.24$  GeV



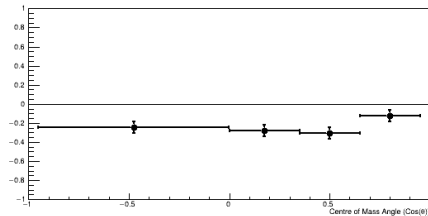


# (Backup) Initial Results, G on $K^+\Sigma$

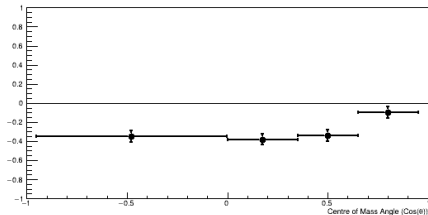
G for  $K\Sigma$  at  $W = 1.77$  to  $1.87$  GeV



G for  $K\Sigma$  at  $W = 1.87$  to  $1.97$  GeV



G for  $K\Sigma$  at  $W = 1.97$  to  $2.06$  GeV



G for  $K\Sigma$  at  $W = 2.06$  to  $2.15$  GeV

